nature communications

Article

https://doi.org/10.1038/s41467-025-61561-z

Methanetetrol and the final frontier in ortho acids

Received: 10 October 2024

Accepted: 20 June 2025

Published online: 14 July 2025

Check for updates

Joshua H. Marks[1,2], Xilin Bai[3], Anatoliy A. Nikolayev[4], Qi'ang Gong[3], Mason McAnally[1,2], Jia Wang[1,2], Yang Pan[5], Ryan C. Fortenberry[6] ✉, Alexander M. Mebel[7] ✉, Tao Yang[3] ✉ & Ralf I. Kaiser[1,2] ✉

The rapid dissociation of methanetetrol ($C(OH)_4$) has been suggested as an impediment to its observation, despite the stability of its substituted derivative orthocarbonates ($C(OR)_4$). Here, the tunability of synchrotron-generated vacuum ultraviolet light and the sensitivity of photoionization are exploited to probe the exotic chemistry of the interstellar medium toward the discovery of this molecule. Laboratory-made model ices simulate the composition of astrophysical ices under conditions mimicking those found in dense interstellar molecular clouds with low temperature (5–10 K) and low pressure ($<10^{-10}$ Torr). High-energy irradiation simulates secondary electrons produced by galactic cosmic rays, one of few sources of energy that penetrate to the icy cloud interior. The reaction mechanism that yields methanetetrol is conclusively revealed by the simultaneous production and detection of key intermediates: carbonic acid (HOCOOH) and the recently reported methanetriol. State-of-the-art electronic structure calculations support the experimental observations and results suggest that if carbonic acid is sufficiently abundant in space, then methanetetrol may be waiting to be observed. The detection of methanetetrol in space-simulation experiments demonstrates that the interstellar medium is host to an unanticipated and counterintuitive chemistry that demands scientific attention.

Despite Wilke's postulation of the existence of the methanetetrol (orthocarbonic acid, $C(OH)_4$, **4**) molecule (Fig. 1) – the only alcohol with four hydroxyl groups located on a single carbon atom – over a century ago[1], it has remained elusive until now. The synthesis of methanetetrol has challenged the synthetic and physical organic chemistry communities, despite the stability of the tetravalent CO_4 moiety in simple esters of orthocarbonic acids ($C(OR)_4$, i.e., orthocarbonates), where R represents methyl ($R = CH_3$), ethyl ($R = C_2H_5$), propyl ($R = C_3H_7$), and butyl ($R = C_4H_9$) groups[2]. These orthocarbonates are being explored as environmentally responsible (green) media for both capturing spent solvent and replacing toxic organic antisolvents[3,4]. Furthermore, the robustness of this group lends to its use in adhesive applications from dentistry to industry[5–8]. Why then has the simplest member of the orthocarbonates – methanetetrol ($R = H$) – never been observed?

In solutions of carbon dioxide (CO_2) in water (H_2O), i.e., carbonated water, carbon dioxide is hydrated to carbonic acid (H_2CO_3, **1**). This is an equilibrium process that is so heavily weighted toward carbon dioxide at ambient temperature, that less than one in one-thousand carbon dioxide molecules is hydrated[9]. However, there has

[1]Department of Chemistry, University of Hawaii at Manoa, Honolulu, HI, USA. [2]W. M. Keck Research Laboratory in Astrochemistry, University of Hawaii at Manoa, Honolulu, HI, USA. [3]State Key Laboratory of Precision Spectroscopy, East China Normal University, Shanghai, PR China. [4]Samara National Research University, Samara, Russia. [5]National Synchrotron Radiation Laboratory, University of Science and Technology of China, Hefei, Anhui, PR China. [6]Department of Chemistry & Biochemistry, University of Mississippi, University, Oxford, MS, USA. [7]Department of Chemistry and Biochemistry, Florida International University, Miami, FL, USA. ✉e-mail: r410@olemiss.edu; mebela@fiu.edu; tyang@lps.ecnu.edu.cn; ralfk@hawaii.edu

https://doi.org/10.1038/s41467-025-61561-z

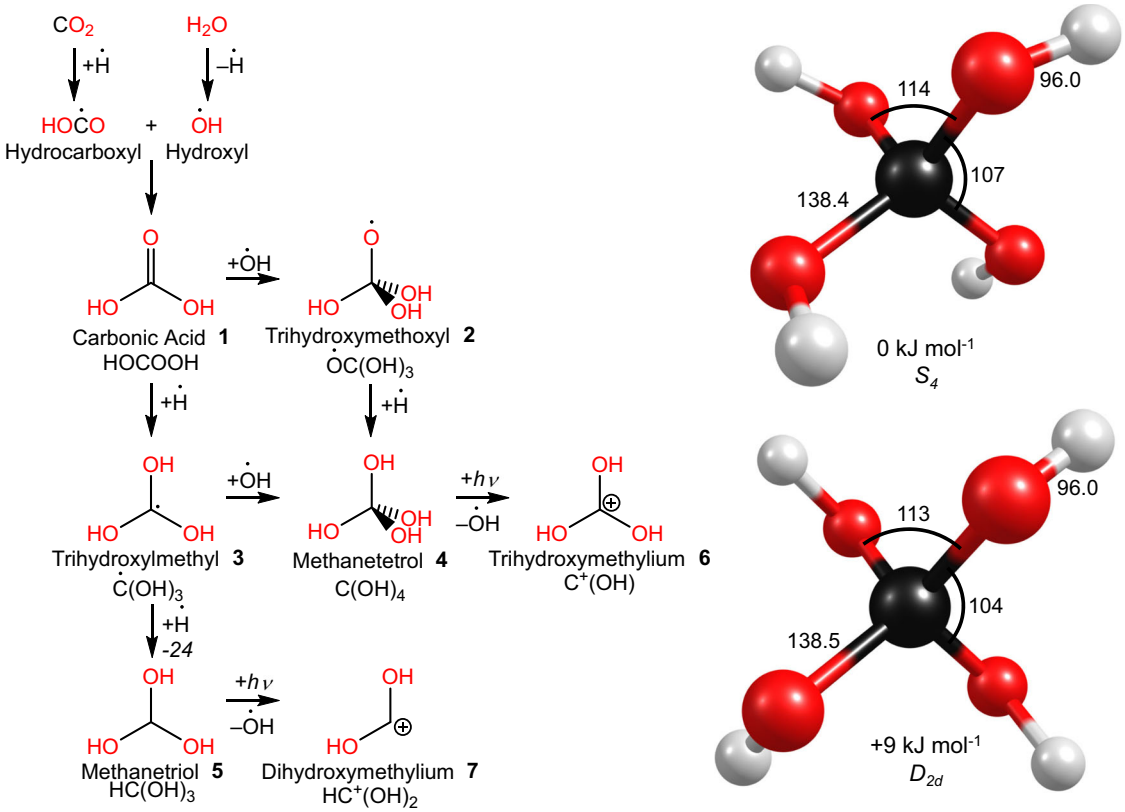

Fig. 1 | Reactions of carbon dioxide (CO_2) and water (H_2O). This reaction scheme describes the formation of carbonic acid (**1**), methanetetrol (**4**), and methanetriol (**5**) by sequential radical-neutral and radical-radical reactions. Only two conformers of **4** are predicted to be stable (right; colored with black carbon, gray hydrogen, and red oxygen) at the highest level of theory employed (CCSD(T)/CBS//ωB97X-D/aug-cc-pVTZ).

been no evidence that carbonic acid (H_2CO_3) can undergo secondary hydration to yield methanetetrol. The Erlenmeyer Rule suggests that organic compounds carrying more than one hydroxyl group at the same carbon atom are thermodynamically not stable and decompose through the elimination of a water molecule and formation of a carbonyl moiety due to the enhanced binding energy of the carbon-oxygen double bond versus two carbon-oxygen single bonds[10]. Additionally, the mutual steric repulsion of the four hydroxyl groups and eight non-bonding electron pairs leads to destabilization.

One approach toward identifying this molecule is the implementation of computational quantum chemistry as a predictive tool toward the stability of methanetetrol, the dissociative barrier that keeps it intact, and the energy liberated by its dissociation[11–19]. Condensed-phase theoretical studies have suggested that it exists as a transient species at temperatures of 4000 K and pressures exceeding 50 GPa, conditions readily achievable in explosive detonations[11]. It is not until pressures greater than 314 GPa are achieved, more than three-million times atmospheric pressure, that methanetetrol is predicted to exist as a stable crystalline polymorph in carbon dioxide-water mixtures[13]. In the isolation of cold vacuum, this still represents a high-energy structure, requiring 83 kJ mol^{-1} for its endoergic formation from carbon dioxide and water with aqueous solvation, which increases both the energy needed and barrier to this reaction[20]. However, isolated gas-phase methanetetrol is kinetically stable and faces a significant barrier of 142 kJ mol^{-1} toward its unimolecular decomposition to water and carbonic acid. Therefore, computations predict that it can be prepared in a suitably isolated environment, where its decomposition is unfavorable. Methanetetrol is also of fundamental interest from the perspective of electronic structure theory and chemical bonding, benchmarking molecular stability, chemical reactivity, and unconventional bond-breaking processes in extreme environments such as low-temperature interstellar molecular clouds (10 K)[21]. As of now, free methanetetrol represents the most elusive alcohol in chemistry, and may be derived from carbonic acid, which was only recently detected in the interstellar medium (ISM)[22].

The first astronomical detection of carbonic acid demonstrates a column density of $(6.4 \pm 0.4) \times 10^{12}$ cm^{-2} and an abundance relative to molecular H_2 of 4.7×10^{-11} toward the molecular cloud G + 0.693–0.027, part of the Sagittarius B2 (Sgr B2) complex located in the central molecular zone of the galaxy[22]. Its discoverers, the team of Rivilla and coworkers, point to the large dipole moment of the *syn-anti* conformer of carbonic acid as aiding in its detection through rotational emission[22]. The *syn-syn* conformer has not yet been detected in space, but because of its low dipole moment the upper limit for its abundance is 25 times that of the more stable *syn-anti* conformer. The cold interstellar molecular cloud environment in which this and many other molecular observations have taken place may be ideal to produce complex or unstable molecules. The nanoparticle-sized grains that comprise these clouds are coated in an icy mantle composed of frozen volatile material and are continuously exposed to high-energy irradiation by the secondary particles produced in the track of a galactic cosmic ray (GCR).

Here, we reveal the very first preparation to the best of our knowledge of the hitherto unreported methanetetrol ($C(OH)_4$, **4**) through exposure of low-temperature (5 K) carbon dioxide–water (CO_2–H_2O) ices to energetic electrons (Supplementary Materials) in a space-simulation experiment. Identification of methanetetrol in the gas phase is accomplished via synchrotron vacuum ultraviolet (SVUV) photoionization (PI) of molecules subliming from the exposed ices during temperature-programmed desorption (TPD). Ions are then mass-analyzed with reflectron time-of-flight mass spectrometry (Re-ToF-MS)[23]. Electronic structure calculations predict isomer-selective

https://doi.org/10.1038/s41467-025-61561-z

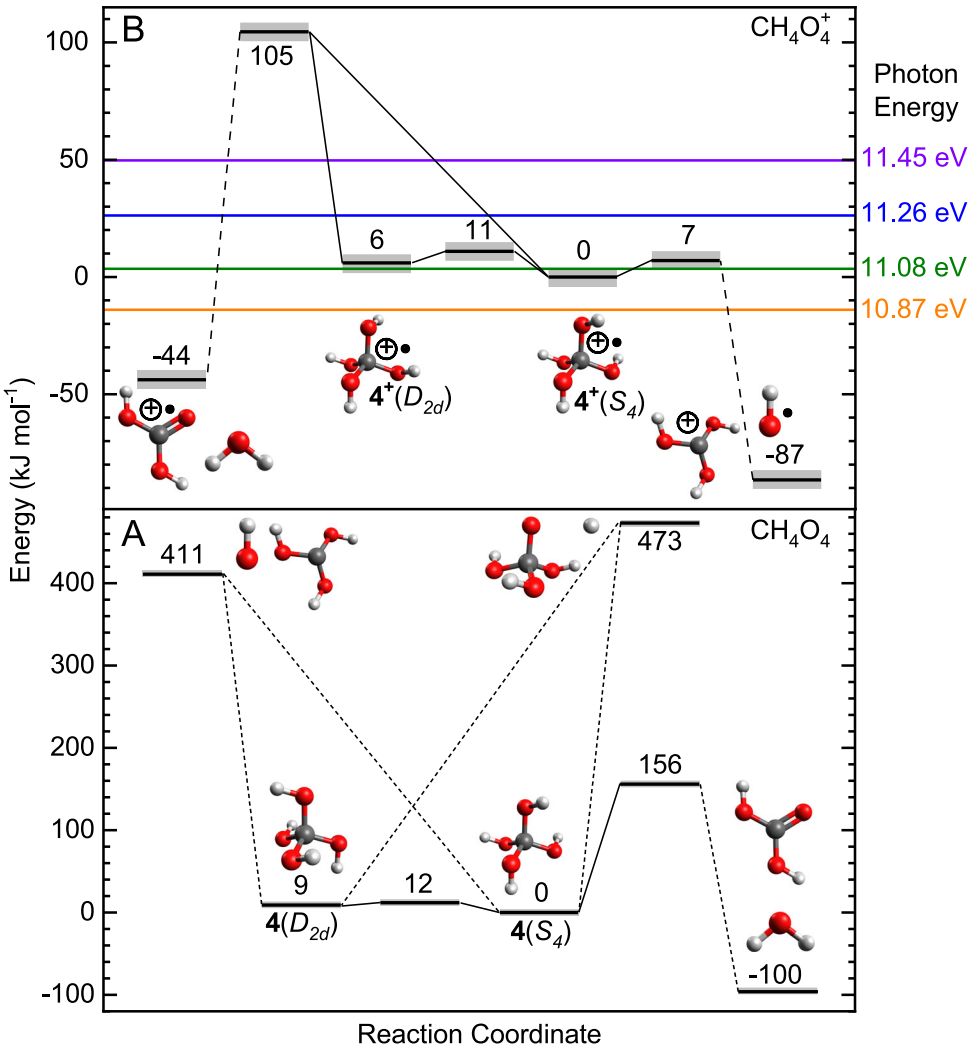

Fig. 2 | Methanetetrol's potential energy surface. Gas-phase potential energy surfaces for (**A**) $C(OH)_4$ (in singlet electronic state) and (**B**) $C(OH)_4^+$ (in doublet electronic state). Energies relative to the minimum energy S_4 conformer of each charge state include an associated error of ±4 kJ mol^{-1} indicated by the gray area. All solid lines connecting energy levels indicate isomerization while dashed lines represent dissociative reaction pathways. Experimental photon energies are indicated with colored horizontal lines.

dissociative photoionization pathways of methanetetrol to trihydroxymethylium ($C(OH)_3^+$, **6**). Along with methanetriol ($HC(OH)_3$, **5**), methanetetrol is ultimately formed via sequential hydrogen atom (H) addition and radical-radical recombination reactions (Figs. 1 and 2) from carbonic acid (H_2CO_3, **1**), thus affording a glimpse at the exotic chemistry leading to molecule **4** in space simulation experiments. Detection of **4** in this environment demonstrates the potential of interstellar chemistry to follow reaction pathways dependent on low temperatures and pressures—inaccessible on Earth outside of a space-simulation chamber—highlighting the need to develop computational and experimental methods needed to explore interstellar chemistry both in the lab and through observation of space.

Results

Our calculations exploring the gas-phase stability of methanetetrol (**4**) were intended to determine if and how it can be detected by photoionization. The neutral molecule must be stable in the gas phase for its photoionization to take place, and with the possible dissociation of the radical cation following photoionization it is essential to anticipate the mass and molecular formulae of fragments. This analysis was performed at the highest feasible level of theory (CCSD(T)/CBS//ωB97X-D/aug-cc-pVTZ)[24–28], and verify previous lower-level computations[14–20,29] and describe a stable neutral gas-phase molecule with a barrier of 156 ± 4 kJ mol^{-1} toward unimolecular dehydration (Fig. 2) to carbonic acid (**1**) (Data S1–S3, Figs. S1–S7)[30–32]. The dissociation of the C–O and O–H bonds of methanetetrol (S_4) are endoergic by 411 ± 4 kJ mol^{-1} and 473 ± 4 kJ mol^{-1}, respectively. While the S_4-symmetric methanetetrol can dehydrate directly, the D_{2d}-symmetric conformer must first interconvert to S_4. However, the interconversion between the two conformers differing in their point group symmetries is effectively barrierless. Despite the relatively low barrier posed by dissociation via dehydration, this process remains thermodynamically inaccessible as represented by these gas-phase calculations. If a Maxwell-Boltzmann distribution of energy is assumed, the average internal energy of any molecule of **4** is expected to be equal to $\frac{2}{\sqrt{\pi}}RT$ where R is the ideal gas constant and T is the temperature. Even at room temperature, the energy available (2.8 kJ mol^{-1}) is far too small for this species to be able to access thermal dissociation.

The purported stability of neutral methanetetrol stands in stark contrast to the instability identified here in the first computational investigation in its radical cation, $C(OH)_4^{+\bullet}$ ($\mathbf{4}^{+\bullet}$). The presence of nonbonding electrons in substituents – i.e., hydroxyl (– OH) – on a carbon atom tends to weaken the other bonds to that carbon when in the radical cation state. The combined effects of all four hydroxyl groups

acting to weaken all neighboring C–O bonds mean that there may be no covalently-bound quantum state for this radical cation. Thermodynamic stability derived from separation of the radical and cation characters into fragments is assisted by the ability of oxygen to donate electron density to partially delocalize the electrostatic charge on the neighboring carbon (hyperconjugation)[33]. The D_{2d} conformer of $C(OH)_4^{+\bullet}$ is prevented from dissociation by a barrier of only 5 ± 4 kJ mol^{-1}, and the contributions to internal energy from heat and photoionization make it likely that the trihydroxymethylium ($C(OH)_3^+$) fragment will be formed upon ionization. However, dissociative photoionization can be taken advantage of because this fragment and its response to photon energy serve as a fingerprint for the presence of methanetetrol. These computational results predict that photon energies above the threshold for dissociative photoionization (11.45 & 11.26 eV) should result in production of the fragment if it is present in the gas phase. Absorption of photons at the threshold (11.08 eV) may plausibly form $C(OH)_4^+$ and presents the best opportunity to detect $C(OH)_4^{+\bullet}$, but below this energy (10.87 eV) photoionization and dissociation cannot proceed.

Only with a priori knowledge of the ionization energy and fragmentation dynamics provided by the preceding computations can meaningful experiments be planned to detect methanetetrol (**4**). Ices composed of carbon dioxide and water (CO_2–H_2O) were subjected to low temperature (<10 K) and pressures (<10^{-10} Torr), i.e., conditions representative of a dense molecular cloud[34–37]. These ices were either unirradiated (blank) or exposed to energetic electrons emulating the action of secondary electrons produced by the passage of a GCR resulting in an energetic dose of 120 ± 10 eV molecule^{-1} CO_2 and 50 ± 5 eV molecule^{-1} H_2O. TPD simulates the warming experienced by clouds during star-formation and is combined with photoionization mass spectrometry at 10.87, 11.08, 11.26, and 11.45 eV (Fig. 3) to detect product species only when the energy is greater than a molecule's adiabatic ionization energy[23,38].

In the blank experiments, no ions were detected showing that any signal observed from irradiated ices is the result of initiated chemistry. Irradiated ices were found to produce signal at $m/z = 47$, which in ices containing only C, H, and O can only have the molecular formula $CH_3O_2^+$. One source of this fragment is methanetriol (**5**) which has no stable cation. However, **5** rather undergoes dissociative photoionization to yield ȮH and $HC(OH)_2^+$ ($m/z = 47$) which is detected by the mass spectrometer; this process requires a reported experimental energy of 11.00–11.08 eV[10]. Fig. 4A shows the signal observed at $m/z = 47$, which is detected at a photon energy of 11.08 eV and above, but not at 10.87 eV. The sublimation profile demonstrated by this fragment is unusual in that it appears to have three separate peaks; however, these peaks all coincide with sublimation of a major component of the ice. The most intense peak at 170 K is the result of **5** co-subliming with H_2O, the peak at 220 K is similar to the sublimation temperature (205 K) reported for **5**[10], and the peak at 250 K appears alongside another intense peak at $m/z = 62$ which is likely carbonic acid (**1**).

The predicted observable ionization energy of the minimum energy conformer of *syn-syn*-carbonic acid is 11.16 ± 0.04 eV and that of the *syn-anti* conformer is 11.09 ± 0.04 eV. While there is predicted to be an *anti-anti* conformer, it is expected to be metastable and short-lived at 220 K (Table S2). The two stable conformers should then be detectable with photon energy of 11.26 eV, but not at 11.08 eV. This predicted response to photon energy is what is observed for carbonic acid (Fig. 4B), but the assignment of the molecular origin of this signal requires more information about the chemical formula(e). In ices composed of only C, H, and O it is possible for this mass (62 amu) to arise from the molecular formulae CH_2O_3, $C_2H_6O_2$, and C_5H_2, and isotopic substitution experiments are necessary for final identification.

If methanetetrol is present, then its $C(OH)_3^+$ fragment ($m/z = 63$) should be observable with photon energies at 11.45 and 11.26 eV. With 11.08 eV photons—at the threshold for dissociative photoionization—it is not clear whether fragmentation must take place. Photons at 10.87 eV are incapable of producing either the molecular radical cation or its cationic fragment. The natural abundances of D, ^{13}C, and ^{17}O means that 1.21% of carbonic acid exists as an isotopomer that weighs 1 amu more and would appear at $m/z = 63$. With photoionization at 11.45 and 11.26 eV, the strong signal from carbonic acid contributing to $m/z = 63$ must be corrected for. After applying this correction, the peak at $m/z = 63$ remains (Fig. 4C). With photoionization at 11.08 eV, a small signal is still observed for $m/z = 63$, and photoionization of carbonic acid does not proceed at this photon energy and therefore its isotopomers cannot be a source of this signal. At this photon energy no signal is observed for the intact cation ($m/z = 80$), indicating that if methanetetrol is the source of this signal it does not exist for long enough or in quantities sufficient for detection. Signal is observed here because the calculations are limited in their accuracy (±4 kJ mol^{-1}) relative to the height of the barrier (7 kJ mol^{-1}), and the internal vibrational energy of these molecules is a distribution with a non-negligible number of molecules energetic enough to surmount the barrier after photoionization. Finally, no signal is observed at 10.87 eV, below the methanetetrol ionization energy. It should also be noted that the sublimation temperature of CH_3OH is 130 K, that of $H_2C(OH)_2$ has been reported as 180 K, that of methanetriol has been observed to be 205 K in the absence of matrix co-sublimation, and the sublimation of methanetetrol at or near 250 K agrees with this pattern of increasing sublimation temperatures as the number of hydroxyl groups rises. While it is tempting to assign this feature to methanetetrol based on its demonstrated behavior, there remains a remote possibility that this signal is due to $C_5H_3^+$ ($m/z = 63$) which can only be addressed with isotopic labeling.

In combination with mass spectrometry, isotopic substitution permits clear identification of a molecular formula. Ices comprising $^{13}CO_2$–H_2O and CO_2–D_2O were studied with 11.26 eV photoionization to verify that the isotopic-mass shift coincides with the correct molecular formula (Fig. 5A). For the fragment of **5**, dihydroxymethylium ($HC(OH)_2^+$), inclusion of ^{13}C shifts the peak to $m/z = 48$ confirming the presence of one carbon atom. Substitution with D shifts the peak to $m/z = 50$ confirming the presence of three H atoms in this fragment and demonstrating that this detection represents both the expected molecular formula (CH_3O_2) and dissociative photoionization threshold of methanetriol, verifying its production here. As for carbonic acid, use of $^{13}CO_2$ increases the mass of the peak by 1 amu showing that only one C is present, and D substitution increases the mass by 2 amu, confirming the molecular formula of **1** to be CH_2O_3 (Fig. 5B). Finally, the peak for the fragment of methanetetrol can be deemed to have the molecular formula $C(OH)_3^+$; ices of $^{13}CO_2$–H_2O reproduce this peak at $m/z = 64$ and CO_2–D_2O ices reproduce this peak at $m/z = 66$, confirming the presence of one carbon and three hydrogen atoms which with 63 amu can only be $C(OH)_3^+$ (Fig. 5C).

Discussion

While the underlying reactions cannot be observed in real-time during these experiments, the species observed through PI-ReToF-MS inform us of the likely mechanism leading to methanetetrol (**4**). These reactions begin in an ice composed exclusively of CO_2 and H_2O, and while concerted hydration of CO_2 to form carbonic acid (**1**) is possible at room temperature in liquid water, i.e., soda water, it is unphysical at 5 K. Rather, the mobility of suprathermal atomic hydrogen within the ice makes dissociation of the O–H bond in reaction [1a] the most active available chemical pathway[39,40]. Where the impinging electron provides the energy to initiate the elimination of atomic hydrogen (Ḣ) from H_2O, the capture by CO_2 in reaction [1b] completes the second half of an endoergic hydrogen transfer reaction. Radical-radical recombination of hydroxycarbonyl (HOĊO) with the remaining

https://doi.org/10.1038/s41467-025-61561-z

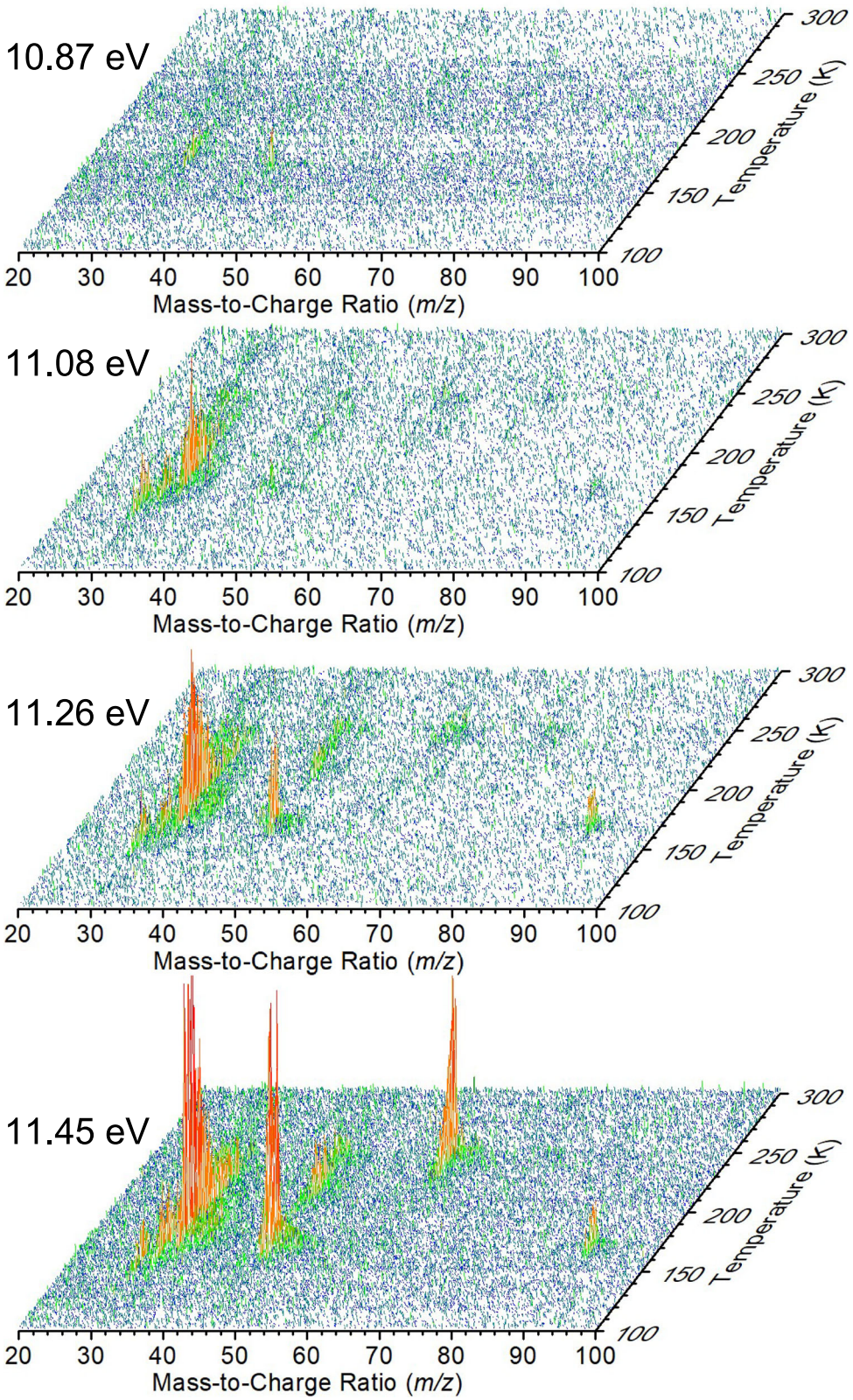

Fig. 3 | Photoionization time-of-flight mass spectrometry (PI-ReToF-MS). During temperature-programmed desorption (TPD), molecules subliming from irradiated CO_2–H_2O ices are photoionized and mass-analyzed. Ion counts recorded at 11.45 eV, 11.26 eV, 11.08 eV, and 10.87 eV during PI-ReToF-MS experiments are shown as a function of temperature and mass-to-charge ratio.

hydroxyl radical (ȮH) then yields carbonic acid (**1**).

$$H_2O \rightarrow \dot{O}H + \dot{H} \quad \Delta H_{react.}{}^{41} = +492.22 \pm 0.04\ \mathrm{kJ\,mol^{-1}} \qquad (1a)$$

$$CO_2 + \dot{H} \rightarrow HO\dot{C}O \quad \Delta H_{react.}{}^{41} = -4.1 \pm 0.4\ \mathrm{kJ\,mol^{-1}} \quad \Delta E_{TS}{}^{42} = 25 \pm 1,\ \mathrm{kJ\,mol^{-1}} \qquad (1b)$$

https://doi.org/10.1038/s41467-025-61561-z

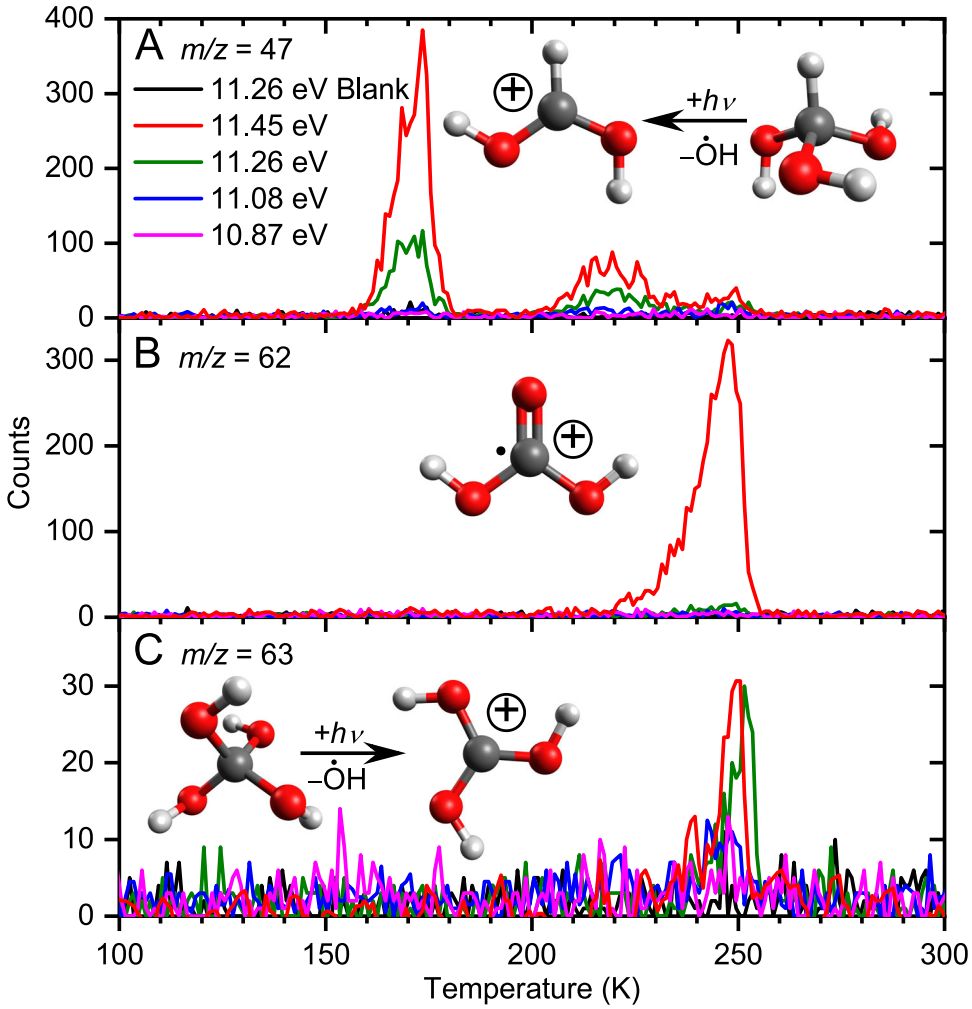

Fig. 4 | Observation of methanetetrol in gas phase. TPD profiles measured for **A** the dissociative photoionization product ($CH(OH)_2^+$) of methanetriol ($CH(OH)_3$), **B** carbonic acid (HOCOOH), and **C** the dissociative photoionization product ($C(OH)_3^+$) of methanetetrol ($C(OH)_4$).

$$\dot{O}H + HO\dot{C}O \rightarrow HOCOOH\,(1) \quad \Delta H_{react.}{}^{41} = -455.452 \pm 0.7\ kJ\ mol^{-1} \tag{2}$$

This surface reaction toward the production of carbonic acid has been suggested as an alternative pathway in the interstellar medium[41–43].

The reaction mechanisms of energetic radical transfer and radical-radical recombination are both accessible at the temperatures and radiation conditions of the ISM. These reactions are sufficiently active that the infrared spectrum of **1** can be easily measured after sublimation of the CO_2 and H_2O matrix (Fig. S9). Experiments in which the infrared spectra were recorded during TPD of irradiated ice demonstrate that at 200 K only **1** remains detectable within the ice[44,45]. A recent publication identifies infrared absorptions in matrix isolation unique to the *cis-cis* conformer centered at 1790 cm^{-1} while the less stable *cis-trans* conformer absorbs at 1830 cm^{-1}[46]; however, these absorption bands cannot be used for conformational assignment here because the peak observed is red-shifted to a center at 1720 cm^{-1} and broadened to a full-width half-maximum of 80 cm^{-1} by molecule-ice interactions. It is most likely that the ice of **1** observed here is amorphous and contains many or all possible conformers of carbonic acid, though the detection of carbonic acid through optical spectroscopy is itself evidence of its efficient production.

The abundance of **1** produced by irradiation leads to an enhanced likelihood of forming second-generation products as the irradiation dose increases. The most abundant radicals in the ice are overwhelmingly likely to be those coming from [1a] and [1b], so transfer of the resulting radicals to **1** are considered in reactions [3a] and [3b]. The two resulting high-energy radical intermediates, trihydroxymethoxyl ($\dot{O}C(OH)_3$, **2**) and trihydroxymethyl ($\dot{C}(OH)_3$, **3**), respectively. Subsequent barrierless radical-radical recombination of **2** with Ḣ yields methanetetrol (**4**), while **3** may undergo recombination with ȮH in reaction [5a] to yield **4** or recombination with Ḣ in [5b] to yield methanetriol (**5**).

$$HOCOOH\,(1) + \dot{O}H \rightarrow \dot{O}C(OH)_3(2) \quad \Delta H_{react.} = +11 \pm 4,\ kJ\ mol^{-1},\ \Delta E_{TS} = 66 \pm 4,\ kJ\ mol^{-1} \tag{3a}$$

$$HOCOOH\,(1) + \dot{H} \rightarrow \dot{C}(OH)_3(3) \quad \Delta H_{react.} = 23 \pm 4,\ kJ\ mol^{-1},\ \Delta E_{TS} = 72 \pm 4,\ kJ\ mol^{-1} \tag{3b}$$

$$\dot{O}C(OH)_3(2) + \dot{H} \rightarrow C(OH)_4(4) \quad \Delta H_{react.} = -472 \pm 4,\ kJ\ mol^{-1} \tag{4}$$

$$\dot{C}(OH)_3(3) + \dot{O}H \rightarrow C(OH)_4(4) \quad \Delta H_{react.} = 446 \pm 4,\ kJ\ mol^{-1} \tag{5a}$$

https://doi.org/10.1038/s41467-025-61561-z

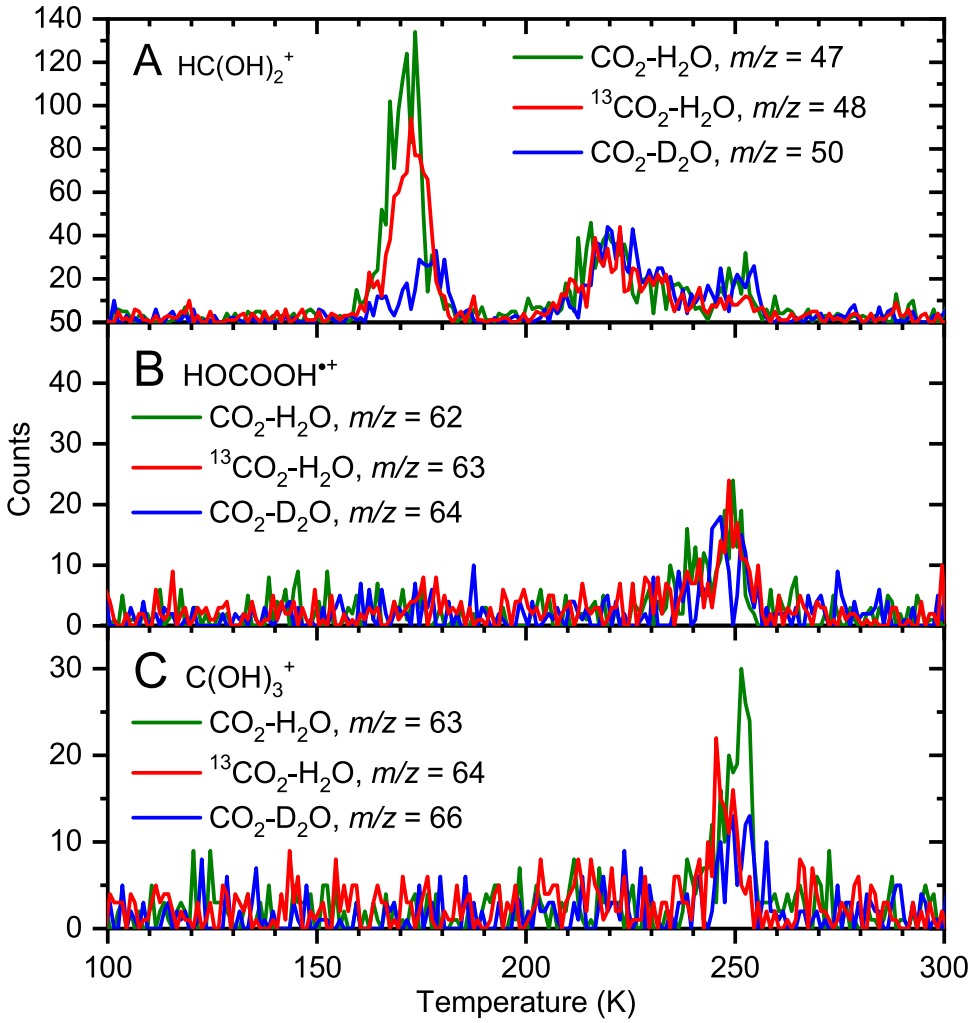

Fig. 5 | Confirming the chemical formulae. TPD profiles measured at 11.26 eV with isotopically substituted ices for **A** the dissociative photoionization product ($CH(OH)_2^+$) of methanetriol ($CH(OH)_3$), **B** carbonic acid (HOCOOH), and **C** the dissociative photoionization product ($C(OH)_3^+$) of methanetetrol ($C(OH)_4$).

$$\dot{C}(OH)_3(3) + \dot{H} \rightarrow HC(OH)_3(5) \quad \Delta H_{react.} = 474 \pm 4, \text{kJ mol}^{-1} \qquad (5b)$$

The overall mechanisms by which **4** and **5** are formed require four discrete steps because at 5 K radical chemistry is all that is available for reaction of neutral species. These reaction steps are separated rather than a concerted mechanism because suprathermal motion of Ḣ through the ice is facilitated by its small size and the large amount of energy imparted by the energetic electrons[39,40]. This means that the H_2O and CO_2 that produce the radicals in [1a] and [1b] that ultimately form **1** need not be nearest neighbors in the ice matrix. Since Ḣ and ȮH radicals are reactants in reactions [2]–[5b], their relative mobility within the ice should be a major determining factor in branching ratios. These radicals compete to consume **1** in reactions [3a] and [3b] and to consume **3** in reactions [5a] and [5b]. The smaller size of Ḣ reduces its collision cross-section and its low mass (1 amu) relative to ȮH means that Ḣ is ejected with more kinetic energy than ȮH during the dissociation event. Conservation of momentum requires that in isolation the dissociated products of reaction [1a] have equal but opposite moments of inertia after dissociation. This results in the Ḣ receiving seventeen times the momentum and therefore the velocity of the ȮH fragment. A targeted computational investigation of the barriers and rate constants of reactions [3]–[5] that considers tunneling and the effects of the icy matrix should prove informative for astrochemical modeling. In particular, the effect of quantum tunneling of radicals at the low temperatures (10 K)[37] found inside dense molecular clouds has the potential to significantly impact reaction rates and the branching ratio of reactions [3a] and [3b] or [5a] and [5b]. The low mass of Ḣ permits tunneling and reactions may occur at even these temperatures, while the mass of ȮH all but precludes its reaction through tunneling at any but astronomical timescales, and therefore must be considered here.

Like reactions limited by mixing rates or diffusion, reactions in the ice may be limited by the rate of suprathermal transport of energetic radicals to their reaction partners[39,40]. The barrier imposed by transition state energy for reaction [3a] and [3b] are similar, but the unequal partitioning of energy during dissociation based on energy and angular momentum conservation means that Ḣ is more likely to be able to overcome this barrier. Consequently, reactions of Ḣ are expected to be far more efficient than competing reactions of ȮH. In terms of ionization energies, dissociative photoionization dynamics, and structures **4** and **5** are very similar. Despite this, there appears to be far more of **5** detected in these experiments (Fig. 4), which is likely due to the superior ability of Ḣ to overcome transition state energetic barriers. The only previous environment in which **5** has been detected was mixed methanol–molecular oxygen (CH_3OH–O_2) ice[10], but the simplified mechanism of formation afforded by CO_2–H_2O ice requires only Ḣ transfer and is at least an order of magnitude more efficient. Within the context of astronomical ices, these findings indicate that irradiation doses of 0.1–1.0 eV amu^{-1} received by molecular clouds

during their 10–50 × 10^6 year collapse into stars and planets should readily yield **1**; but these doses may represent too modest exposures to instigate the formation of **4**[47]. In contrast, cometary and planetary ices continue to undergo GCR irradiation in addition to solar photolysis, and these ices are more likely to host molecules like **4** and **5**.

The production of methanetetrol ($C(OH)_4$, **4**) marks the introduction of the most elusive, previously unreported member of the hydroxymethanes ($H_nC(OH)_{n-4}$) to the chemistry community. Though methanol (H_3COH) is common and methanediol ($H_2C(OH)_2$) is known as an aqueous form of formaldehyde (H_2CO), methanediol had not been identified in the gas phase until as recently as 2022[48]. Conversely, methanetriol[10] ($HC(OH)_3$, **5**) had never been observed until earlier last year, nor had methanetetrol, though now both have been reported in the gas phase. The observation of efficient production of methanetriol from carbonic acid (HOCOOH, **1**) has the potential to instigate new lines of research in spectroscopy, astrochemistry, and astronomy. Spectral and chemical information is needed as a prerequisite to deploying modern astronomical techniques to identify molecules like methanetetrol in space; however, by mapping the chemical contents of the interstellar medium we gain insight into its evolution. The extremes of the low temperature found within dense interstellar clouds (<10 K) and the high-energy initiation provided by GCRs reveal chemistry that was once inaccessible to science and allow the discovery of molecules in the laboratory and in space.

In these experiments we demonstrate the first detection of methanetetrol while simultaneously identifying intermediates in its radical formation mechanism, carbonic acid and methanetriol. The production of these species in a space simulation experiment raises the prospect of their future observation in the interstellar medium, particularly in star-forming regions where methanetetrol can sublime into the gas phase. Water is the most abundant astronomical ice component and carbon dioxide is present at concentrations of 1–50% relative to water, making the precursors for carbonic acid's formation commonplace throughout interstellar space[49]. The high turbulence, temperatures, and radiation in the central molecular zone, where carbonic acid was identified, appears ideal for its production and may contribute significantly to its abundance[22]. Reactions of this species are shown here to result in the production of both methanetriol and methanetetrol, indicating that these and other such supposedly impossible molecules may be commonplace in the chemistry of the ISM. A direct connection between the production of methanetetrol and, more generally, orthocarbonic acids and chemical pathways toward larger interstellar complex organic molecules influencing the physics and chemistry of the interstellar medium and potentially leading to planet formation and the origins of life is in its infancy. An energetic oxygen chemistry, which is vital for all life, may be traceable by the future detection of methanetetrol in the interstellar medium, particularly toward hot molecular cores such as Sgr B2. Further chemistry derived from methanetetrol can potentially lead to molecules of the $ROC(OH)_3$ structure with R being an organic side group. Finally, methanetetrol and the $ROC(OH)_3$ derivatives could represent a hitherto neglected reservoir of carbonic acid (HOCOOH) and carbonic acid esters (ROCOOH) on interstellar ices. This molecule's identification here represents a blind spot and the lack of its detection to date in the terrestrial environment is evidence of the counter-intuitive chemistry of the interstellar medium and justification for its promotion.

Methods

Synchrotron vacuum ultraviolet photoionization reflectron time-of-flight mass spectrometry (SVUV-PI-ReToF-MS)

Surface scattering experiments utilizing vacuum ultraviolet (VUV) synchrotron radiation were conducted at the Shanghai-Hawaii-Hefei Advanced Research Center (SHHARC) at the National Synchrotron Radiation Laboratory (NSRL) in Hefei, Anhui, China, on the BL03U beamline for astrochemistry (Table S4)[23]. Experiments were conducted in a hydrocarbon-free stainless steel ultra-high vacuum (UHV) chamber and ices are were deposited onto a mirror-polished silver wafer (12.6 × 15.1 mm) maintained at 4.8 ± 0.1 K by a Gifford-McMahon helium cryocooler (Sumitomo Heavy Industries, RDK-415E). Samples were introduced to the chamber and condensed onto the surface of the silver waver using two leak valves (10^{-8} Torr each) that flow gas through glass capillary arrays (10 mm array diameter) directed at the wafer. Samples used include carbon dioxide (CO_2, Nanjing Special Gas Factory Co., 99.999%; $^{13}CO_2$, Cambridge Isotope Laboratories, 99.0% atom ^{13}C) and water (H_2O, Shanghai Macklin Biochemical Technology Co., HPLC grade; D_2O, Shanghai Aladdin Biochemical Technology Co., 99.9% atom D; $H_2{}^{18}O$, Shanghai Aladdin Biochemical Technology Co., 97.0% atom ^{18}O). Prior to experiments using D_2O, all tubing and chambers were purged with D_2O vapor to allow any H/D isotopic exchange between the sample and container to occur prior to experimental ice deposition; this process was repeated with H_2O after use of D_2O. The same procedure for assuring isotopic purity of the sample delivered to the wafer was repeated for experiments using $H_2{}^{18}O$. The thickness of deposited ices was measured based on the reflected intensity of a helium-neon laser (CVI Melles-Griot, 25-LHP-230, 632.8 nm) at a 2° angle of incidence. Variations in reflected laser intensity resulting from thin-film interference during deposition indicate an average ice thickness of 750 ± 50 nm[36]. In calculating this thickness, the ice index of refraction was approximated by the average of the indexes of refraction of the two components, 1.27 ± 0.02 in amorphous ices of both components[34].

For the purpose of simulating the electron irradiation computationally, densities of 0.87 ± 0.03 g cm^{-3} for amorphous H_2O ice[34] and 0.98 ± 0.02 g cm^{-3} for amorphous CO_2 ice[35] were used as an approximation for the unknown density of the mixed ices[34]. Monte Carlo simulations conducted in CASINO 2.42 predict average electron penetration depth, energy transmitted to ice, and energy backscattered from ice surface[38]. The ice thickness is kept significantly greater than the average penetration depth (at which electrons have expended 90% of their energy) to prevent interactions between the ice and the silver substrate from being initiated by the energetic electrons. In these simulations, <0.01% of electrons penetrated the ice to the substrate. Irradiation parameters including dose and ice characterization are detailed in Tables S5 and S6.

Synchrotron vacuum ultraviolet photoionization reflectron time-of-flight mass spectroscopy (SVUV-PI-ReToF-MS) utilized temperature-programmed desorption (TPD) at a rate of 1 K min^{-1} and VUV light that was passed 1–2 mm above the surface of the ice to photoionize subliming molecules[23]. Ions are mass-analyzed in a reflectron time-of-flight mass spectrometer (Jordan TOF Products). The SVUV light is quasi-continuous, requiring pulsed extraction of ions into the mass spectrometer. This was accomplished by electronic pulsing of the extraction grid between a small repelling voltage (1.5 V, 64.2 µs) and an extraction voltage (−150 V, 2.5 µs), where extraction marks the beginning of each cycle of the ReToF-MS. A 40 mm dual-multichannel plate detector (Jordan TOF Products, C-726) is used in an ion-counting scheme comprising preamplification (Ortec, 9305), discrimination & amplification to 4 V (Advanced Research Instruments Corp., F-100TD), and recording by a multichannel scaler (FAST ComTec, P7889) with 3.2 ns accuracy. Mass spectra were repeated at a rate of 15 kHz (66.7 µs per mass spectrum) until the temperature of the sample reached a minimum of 300 K.

Surface scattering machine

Additional experiments were conducted in the surface scattering machine at the University of Hawaii at Manoa, an apparatus consisting of a hydrocarbon-free stainless steel ultrahigh-vacuum chamber. This instrument is nearly identical to the SVUV-PI-ReToF-MS instrument with the substitution of ToF-MS for a Fourier transform infrared spectrometer (FTIR, Thermo, Nicolet 6700) continuously measuring

spectra in the 4000–500 cm^{-1} range with 4 cm^{-1} resolution. Spectra were measured continuously and averaged every two minutes during irradiation and TPD. Subliming molecules were detected during TPD via an electron-impact (100 eV) quadrupole mass spectrometer (EI-QMS, QMG 420) in the residual gas analyzer mode. The measured infrared spectrum, in agreement with that of carbonic acid (**1**), is shown in Fig. S8.

Computational methods

For all molecules except carbonic acid (HOCOOH, **1**), initial geometry optimizations and vibrational frequency analyses including zero-point vibrational energy (ZPVE) corrections were performed with Head-Gordon's long-range corrected hybrid density functional with Dunning's correlation consistent basis set at the ωB97X-D[24]/aug-cc-pVTZ[23,26] level of theory for all neutral molecules in the Gaussian 09 computational package[50]. Accurate electronic energies were obtained by using the optimized structures to carry out single-point coupled cluster explicitly including single, double, and perturbative triple excitations with extrapolation to the complete basis set limit at the composite CCSD(T)[27]/CBS//ωB97X-D/aug-cc-pVTZ level of theory using the MOLPRO 2015 package[51]. Minimum energy structures for cations were initially optimized from the previously final structures of the corresponding neutral molecules to identify the cation structure reached via vertical ionization. After optimization, frequency analysis, and CBS extrapolation were repeated to determine the difference in sum of electronic and ZPVE (CCSD(T)/CBS//ωB97X-D/aug-cc-pVTZ +ZPVE) between the neutral and cationic states, defined here as the adiabatic ionization energy (IE). The same computational methods were employed for all identified transitions and dissociated states investigated. All neutral and cationic structures were confirmed to have all real vibrational frequencies, and all optimized transition states were confirmed to have only one imaginary (negative) frequency corresponding to the reaction coordinate. Investigated structures included all plausible covalently bound and all reasonable non-covalently bound minimum-energy configurations of the CH_4O_4 system of isomers in Figs. S1–S8, and Data S1.

For **1** and its dimer, the neutral and radical cation geometries were optimized with explicitly correlated coupled cluster singles, doubles, and perturbative triples (CCSD(T)-F12) in conjunction with the cc-pVTZ-F12 basis set as available from the MOLPRO 2020.1 program[30]. The harmonic vibrational energies and ZPVEs were also computed at this same level of theory. The relative energies were computed as differences in energy including ZPVEs from the most stable neutral to the given conformer. The adiabatic ionization potentials are computed as the differences between the energies of the optimized neutrals and those of the corresponding optimized radical cations including the ZPVE values, as well (Data S2 and S3). Because these CCSD(T)-F12 calculations were conducted at a different level of theory compared to the composite CCSD(T)/CBS//ωB97X-D/aug-cc-pVTZ method, we conducted benchmarking calculations, the results of which are detailed in the Supplementary Materials in Tables S7–S20 showing close agreement between the two theoretical approaches.

Data availability

All data are available in the main text, the supplementary materials, or upon request to the corresponding authors. The experimental data generated in this study have been deposited in the University of Hawai'i reaction dynamics and materials in extreme environments database at http://uhmreactiondynamics.org/publications.html Correspondence and requests for materials should be addressed to Ralf I. Kaiser.

References

1. Wilke, E. Zur kenntnis wäßriger kohlensäurelösungen. *Z. Anorg. Allg. Chem.* **119**, 365–379 (1922).
2. Tieckelmann, H. & Post, H. W. The preparation of methyl, ethyl, propyl, and butyl orthocarbonates. *J. Org. Chem.* **13**, 265–267 (2002).
3. Wang, M. et al. Systematic optimization of perovskite solar cells via green solvent systems. *Chem. Eng. J.* **387**, 123966 (2020).
4. Gou, Y. et al. Research progress of green antisolvent for perovskite solar cells. *Mater. Horiz.* **11**, 3465–3481 (2024).
5. Xu, X., Wu, Y. & Wang, C. Synthesis of DOPO-based spiroorthocarbonate and its application in epoxy resin. *Des. Monomers Polym.* **18**, 690–697 (2015).
6. Narasimhamurthy, N., Manohar, H., Samuelson, A. G. & Chandrasekhar, J. Cumulative anomeric effect: a theoretical and x-ray diffraction study of orthocarbonates. *J. Am. Chem. Soc.* **112**, 2937–2941 (2002).
7. Sonmez, H. B. & Wudl, F. Cross-linked poly(orthocarbonate)s as organic solvent sorbents. *Macromolecules* **38**, 1623–1626 (2005).
8. Wenthe, A. M. & Cordes, E. H. Concerning the mechanism of acid-catalyzed hydrolysis of ketals, ortho esters, and orthocarbonates. *J. Am. Chem. Soc.* **87**, 3173–3180 (2002).
9. Miessler, G., Fischer, P. & Tarr, D. *Inorganic chemistry* (Pearson, 2013).
10. Marks, J. H. et al. Methanetriol—Formation of an impossible molecule. *J. Am. Chem. Soc.* **146**, 12174–12184 (2024).
11. Xiong, G., Zhu, S., Yang, C. & Zhu, W. Insight into interaction mechanisms of binary mixture systems of explosion products (H_2O, CO_2, and N_2) at extreme high pressures and temperatures. *Chem. Phys. Lett.* **714**, 103–110 (2019).
12. Heard, G. L., Gillespie, R. J. & Rankin, D. W. H. Ligand close packing and the geometries of $A(XY)_4$ and some related molecules. *J. Mol. Struc. THEOCHEM* **520**, 237–248 (2000).
13. Saleh, G. & Oganov, A. R. Novel stable compounds in the C-H-O ternary system at high pressure. *Sci. Rep.* **6**, 32486 (2016).
14. Toumi, I. et al. Stereoisomers of hydroxymethanes: probing structural and spectroscopic features upon substitution. *J. Chem. Phys.* **145**, 244305 (2016).
15. Barić, D. & Maksić, Z. B. Additivity of the correlation energy in some 3D organic molecules. *J. Phys. Chem. A* **106**, 1612–1618 (2002).
16. Gillespie, R. J., Bytheway, I. & Robinson, E. A. Bond lengths and bond angles in oxo, hydroxo, and alkoxo molecules of Be, B, and C: a close-packed nearly ionic model. *Inorg. Chem.* **37**, 2811–2825 (1998).
17. Gillespie, R. J., Robinson, E. A. & Pilme, J. Ligand close packing, molecular compactness, the methyl tilt, molecular conformations, and a new model for the anomeric effect. *Chem. Eur. J.* **16**, 3663–3675 (2010).
18. Gibbs, G. V., D'Arco, P. & Boisen, M. B. Molecular mimicry of bond length and angle variations in germanate and thiogermanate crystals: a comparison with variations calculated for carbon-, silicon-, and tin-containing oxide and sulfide Molecules. *J. Phys. Chem.* **91**, 5347–5354 (2002).
19. Hess, A. C., McMillan, P. F. & O'Keeffe, M. Torsional barriers and force fields in H_4TO_4 molecules and molecular ions (T = carbon, boron, aluminum, silicon). *J. Phys. Chem.* **92**, 1785–1791 (2002).
20. Böhm, S., Antipova, D. & Kuthan, J. A study of methanetetraol dehydration to carbonic acid. *Int. J. Quant. Chem.* **62**, 315–322 (1997).
21. Puzzarini, C. & Alessandrini, S. Interstellar ices: a factory of the origin-of-life molecules. *ACS Cent. Sci.* **10**, 13–15 (2024).
22. Sanz-Novo, M. et al. Discovery of the elusive carbonic acid (HOCOOH) in space. *Astrophys. J.* **954**, 3 (2023).
23. Zhu, C. et al. Exploitation of synchrotron radiation photoionization mass spectrometry in the analysis of complex organics in interstellar model ices. *J. Phys. Chem. Lett.* **13**, 6875–6882 (2022).

24. Chai, J. D. & Head-Gordon, M. Long-range corrected hybrid density functionals with damped atom-atom dispersion corrections. *Phys. Chem. Chem. Phys.* **10**, 6615–6620 (2008).
25. Dunning, T. H. Gaussian basis sets for use in correlated molecular calculations. I. The atoms boron through neon and hydrogen. *J. Chem. Phys.* **90**, 1007–1023 (1989).
26. Kendall, R. A., Dunning, T. H. & Harrison, R. J. Electron affinities of the first-row atoms revisited. Systematic basis sets and wave functions. *J. Chem. Phys.* **96**, 6796–6806 (1992).
27. Stanton, J. F. Why CCSD(T) works: a different perspective. *Chem. Phys. Lett.* **281**, 130–134 (1997).
28. Lee, T. J. & Taylor, P. R. A diagnostic for determining the quality of single-reference electron correlation methods. *Int. J. Quant. Chem.***36**, 199–207 (1989).
29. Lehn, J.-M., Wipff, G. & Bürgi, H.-B. Stereoelectronic properties of tetrahedral species derived from carbonyl groups. Ab initio study of the hydroxymethanes. *Helv. Chim. Acta* **57**, 493–496 (1974).
30. Raghavachari, K., Trucks, G. W., Pople, J. A. & Head-Gordon, M. A fifth-order perturbation comparison of electron correlation theories. *Chem. Phys. Lett.* **157**, 479–483 (1989).
31. Adler, T. B., Knizia, G. & Werner, H. J. A simple and efficient CCSD(T)-F12 approximation. *J. Chem. Phys.* **127**, 221106 (2007).
32. Knizia, G., Adler, T. B. & Werner, H. J. Simplified CCSD(T)-F12 methods: theory and benchmarks. *J. Chem. Phys.* **130**, 054104 (2009).
33. Wang, C., Chen, Z., Wu, W. & Mo, Y. How the generalized anomeric effect influences the conformational preference. *Chem. Eur. J.* **19**, 1436–1444 (2013).
34. Bouilloud, M. et al. Bibliographic review and new measurements of the infrared band strengths of pure molecules at 25 K: H_2O, CO_2, CO, CH_4, NH_3, CH_3OH, HCOOH and H_2CO. *Mon. Not. R. Astron. Soc.* **451**, 2145–2160 (2015).
35. Satorre, M. Á et al. Density of CH_4, N_2 and CO_2 ices at different temperatures of deposition. *Planet. Space Sci.* **56**, 1748–1752 (2008).
36. Turner, A. M. et al. A photoionization mass spectroscopic study on the formation of phosphanes in low temperature phosphine ices. *Phys. Chem. Chem. Phys.* **17**, 27281–27291 (2015).
37. Carroll, B. W. & Ostlie, D. A. *An Introduction to Modern Astrophysics* (Cambridge University Press, 2017).
38. Drouin, D. et al. CASINO V2.42—A fast and easy-to-use modeling tool for scanning electron microscopy and microanalysis users. *Scanning* **29**, 92–101 (2007).
39. Kaiser, R. I. & Roessler, K. Theoretical and laboratory studies on the interaction of cosmic ray particles with interstellar ices. III. Suprathermal chemistry-induced formation of hydrocarbon molecules in solid methane (CH_4), ethylene (C_2H_4), and acetylene (C_2H_2). *Astrophys. J.* **503**, 959–975 (1998).
40. Zheng, W., Jewitt, D. & Kaiser, R. I. Formation of hydrogen, oxygen, and hydrogen peroxide in electron-irradiated crystalline water ice. *Astrophys. J.* **639**, 534–548 (2006).
41. Ruscic, B. & Bross, D. Active thermochemical tables (ATcT) values based on ver. 1.130 of the thermochemical network. Argonne national laboratory, Lemont, Illinois 2023; available at ATcT.anl.gov. https://doi.org/10.17038/CSE/1997229 (2023).
42. Li, J. et al. Communication: a chemically accurate global potential energy surface for the HO + CO → H + CO_2 Reaction. *J. Chem. Phys.* **136**, 041103 (2012).
43. Ioppolo, S. et al. Vacuum ultraviolet photoabsorption spectroscopy of space-related ices: formation and destruction of solid carbonic acid upon 1 keV electron irradiation. *Astron. Astrophys.* **646**, A172 (2021).
44. Jones, B. M., Kaiser, R. I. & Strazzulla, G. Carbonic acid as a reserve of carbon dioxide on icy moons: the formation of carbon dioxide (CO_2) in a polar environment. *Astrophys. J.* **788**, 170 (2014).
45. DelloRusso, N., Khanna, R. K. & Moore, M. H. Identification and yield of carbonic acid and formaldehyde in irradiated ices. *J. Geophys. Res. Planets* **98**, 5505–5510 (1993).
46. Schlagin et al. Solving the puzzle of the carbonic acid vibrational spectrum – An anharmonic story. *ChemPhysChem* **25**, e202400274 (2024).
47. Yeghikyan, A. G. Irradiation of dust in molecular clouds. II. Doses produced by cosmic rays. *Astrophys* **54**, 87–99 (2011).
48. Zhu, C. et al. Synthesis of methanediol [$CH_2(OH)_2$]: the simplest geminal diol. *Proc. Natl. Acad. Sci. USA.* **119**, e2111938119 (2022).
49. Boogert, A. C. A., Gerakines, P. A. & Whittet, D. C. B. Observations of the icy universe. *Annu. Rev.* **53**, 542–581 (2015).
50. Frisch, M. J. et al. Gaussian 09, Revision D.01 (Gaussian, Inc., Wallingford CT, 2009).
51. MOLPRO, Version 2015.1, A package of ab initio programs (University of Cardiff, Cardiff, UK, 2015).

Acknowledgements

This work was conducted under a Memorandum of Understanding between the East China Normal University, the University of Hawaii at Manoa, and the National Synchrotron Radiation Laboratory (NSRL) at the University of Science and Technology of China (USTC). RCF is supported by National Aeronautics and Space Administration grant 80NSSC24M0132 (RCF), National Science Foundation grant AST-2407815 (RCF), with computing resources provided by the Mississippi Center for Supercomputing Research. T.Y. is supported by the National Natural Science Foundation of China grants 12034008 (T.Y.), 12250003 (T.Y.) and 12274140 (T.Y.), the Program for Professor of Special Appointment (Eastern Scholar) at the Shanghai Institutions of Higher Learning, the Young Top-Notch Talent Support Program of Shanghai, Xinjiang Tianchi Talent Program 2023, the Shanghai Natural Science Foundation grant 22ZR1421400 (T.Y.). R.I.K. is supported by National Science Foundation grants AST-2103269 (R.I.K.) & AST-2403867 (R.I.K.) and the equipment was financed by the W. M. Keck Foundation.

Author contributions

The project was supervised by R.C.F., A.M., T.Y., Y.P., and R.I.K. The experiments were designed by J.H.M. and R.I.K. Quantum chemical computations were conducted by A.A.N. and R.C.F. Laboratory astrochemistry experiments were conducted by X.B. and Q.G. Data was analyzed by J.H.M., J.W., and M.M. The manuscript was drafted by J.H.M. with review and editing from A.M.M., T.Y., and R.I.K.

Competing interests

The authors declare no competing interests.

Additional information

Supplementary information The online version contains supplementary material available at https://doi.org/10.1038/s41467-025-61561-z.

Correspondence and requests for materials should be addressed to Ryan C. Fortenberry, Alexander M. Mebel, Tao Yang or Ralf I. Kaiser.

Peer review information *Nature Communications* thanks Dario Campisi and the other, anonymous, reviewer(s) for their contribution to the peer review of this work. A peer review file is available.